

Original Article

# Investigating the Seismic Response of Coupled Isolated Buildings under Stochastic Ground Motions

Dipak Jivani<sup>1</sup>, Ramnik Dhamsaniya<sup>2</sup>

<sup>1</sup>Gujarat Technological University, Gujarat, India.

<sup>2</sup>Department of Civil Engineering, Darshan University, Gujarat, India.

<sup>1</sup>Corresponding Author : [dipak.jivani@darshan.ac.in](mailto:dipak.jivani@darshan.ac.in)

Received: 13 December 2023

Revised: 12 January 2024

Accepted: 13 February 2024

Published: 29 February 2024

**Abstract** - This paper studies the torsional behaviour of a Triple Friction Pendulum (TFP) isolator subjected to stochastic ground motions. Stochastic ground motions are simulated by implementing the Monte Carlo technique. To investigate the torsional response of TFP isolated systems with various superstructure and isolation system eccentricities, along with the superstructures uncoupled torsional to lateral frequency ratio, nonlinear dynamic analyses are carried out. A response of the torsionally uncoupled TFP isolated system is compared with the corresponding response of the torsionally coupled TFP isolated system. Furthermore, a parametric investigation is performed to evaluate the impact of superstructure flexibility on the torsional response of torsionally coupled TFP-isolated buildings. The displacement obtained due to eccentricity in the system is contrasted with the design-bearing displacement recommended by the Uniform Building Code. It has been found that the base-isolated building's seismic response is significantly influenced by the torsional coupling caused by eccentricities at the isolator level. Additionally, when the superstructure time period increases, a rising torsional response of the structure is seen. It is revealed that when isolation eccentricities occur, the impacts of superstructure eccentricity are diminished. The UBC standard's design bearing displacement is considered conservative for the isolation eccentricities.

**Keywords** - Base isolation, Seismic response, Stochastic ground motion, Triple Friction Pendulum isolator, Torsional response.

## 1. Introduction

Extreme loads can cause damage to civil infrastructures such as buildings, roads, and bridges throughout their lifetime. A paramount concern for structural engineers regarding severe loads is earthquake loading. Throughout the past century, severe earthquakes have inflicted extensive and catastrophic damage, primarily attributed to the dynamic movement of the groundmass. This movement often leads to the collapse or severe impairment of infrastructure, accompanied by tragic losses of human life. The inherent difficulty in accurately predicting long-term earthquake occurrences makes it essential to create structures that can resist credible seismic excitation.

The urgent need to develop effective measures for mitigating the devastating impacts of seismic activity has led to the exploration of innovative engineering solutions. Among these, base isolation emerges as a promising earthquake-protecting device. Base isolation is a method that lessens the transfer of horizontal acceleration into the structure by separating it from the ground. It is a seismic design strategy that protects the building from the dangers of earthquake forces by an energy dissipation mechanism and provides horizontal flexibility. The isolation system's flexibility

extends the predominant time period of the structure. It relocates it away from the zone of dominating earthquake frequency contents, while isolation damping improves the energy-absorbing capacity.

A lack of symmetry can have severe negative torsional effects and cause a building to collapse. Eccentricity in the centre of stiffness, mass, or strength produces asymmetry within structures. The best strategy for reducing torsional impacts is to choose regular floor layouts that reduce all eccentricity. However, it would not be practicable because of architectural limitations. An alternative and viable solution is the application of base isolation devices. Due to its ability to dissipate energy and provide flexibility, the base isolation considerably reduces the torsional response of structures during strong earthquakes [15].

Numerous academics have examined the response of base-isolated asymmetrical structures. Jangid and Datta [7-10] and Jangid [6] examined the nonlinear response of torsionally coupled base-isolated structures with various isolation techniques. According to these investigations, torsion in asymmetric structures lowers the isolator's effectiveness compared to symmetric ones. Eccentricity caused by isolators'



superstructure and yield strength dramatically reduces their efficiency. The eccentricity at the isolation level causes the base displacements to increase and the superstructure displacements to somewhat decrease. Soni et al. have studied the response of an asymmetric single-storey structure isolated by a Double Variable Frequency Pendulum Isolator (DVFPI) [18].

They investigated the torsional behaviour under far-fault accelerations to determine the impact of the superstructure period, coefficient of friction, and frequency variation variables. They concluded that the top sliding surface should be softer and smoother than the bottom one to maximize the performance of the DVFPI. The effects of torsional coupling on the seismic performance of base-isolated structures using laminated rubber bearings, lead rubber bearings, and friction pendulum-isolated systems were examined by Matsagar and Jangid [12, 13]. It was found that a torsionally flexible system exhibits a more excellent displacement response than a torsionally rigid one. Additionally, they investigated the dynamic behaviour of base-isolated asymmetric structure considering an impact with adjacent structure. It was discovered that - as eccentricity increases, the torsional response worsens.

Since triple friction pendulum isolation represents the most recent advancement in seismic isolation technology among all base-isolation systems created to date, it is the subject of this study. The key benefit of triple friction base isolators is their efficiency over a broad range of frequency inputs and their huge displacement capacity [4, 5]. Past researchers have presented a comprehensive investigation of various isolation systems and their implementation, and the same was published by Buckle et al. [1] and Naeim and Kelly [14].

Under stochastic ground motion, the torsional behaviour of an asymmetric building isolated by a triple friction isolator bearing has not yet been studied. This is critical because the Triple Friction Pendulum (TFP) bearing is one of the current strategies for enhancing the structure's seismic performance and, hence, must be evaluated for effectiveness under stochastic ground motion. Most constructions are also asymmetrical, which can have negative consequences and cause a building to collapse. Hence, this work examines the seismic response of a one-storey, asymmetric structure to stochastic ground motions. The study aims are:

1. To explore the torsional response of Triple Friction Pendulum bearing (TFP) subjected to stochastic ground motions.
2. To study the impact of superstructure and isolation eccentricities on the response of the TFP isolated system.
3. To conduct a parametric study to assess the impact of superstructure flexibility on the behaviour of the TFP isolated building.

The various factors considered include the eccentricity ratio of the superstructure, the eccentricity ratio at the level of the isolator, the uncoupled time period, and the uncoupled torsional to lateral frequency ratio.

## 2. Triple Friction Pendulum Isolator Mathematical Model

The conventional TFP bearing, which Fenz and Constantinou proposed, has three separate pendulum mechanisms and four concave surfaces. In Figure 1, a slice through a typical TFP bearing is displayed. According to Figure 1, the concave plates have radii of curvature as  $\bar{R}_i$ . At sliding interfaces, the sliding capacity and friction coefficient are indicated by the symbols  $\bar{d}_i$  and  $\bar{\mu}_i$ . The articulated slider's pivot point is shown as being at a distance of  $h_i$  from the  $i^{\text{th}}$  spherical surface [4, 5].

These bearings' internal design causes sliding on various combinations of interfaces, which alters stiffness and damping throughout the motion. Two mathematical approaches-the parallel and the series-can be used to predict the behaviour of TFP bearings. The five operational regimes of the TFP bearing can all be described by the series model and are used in the current research.

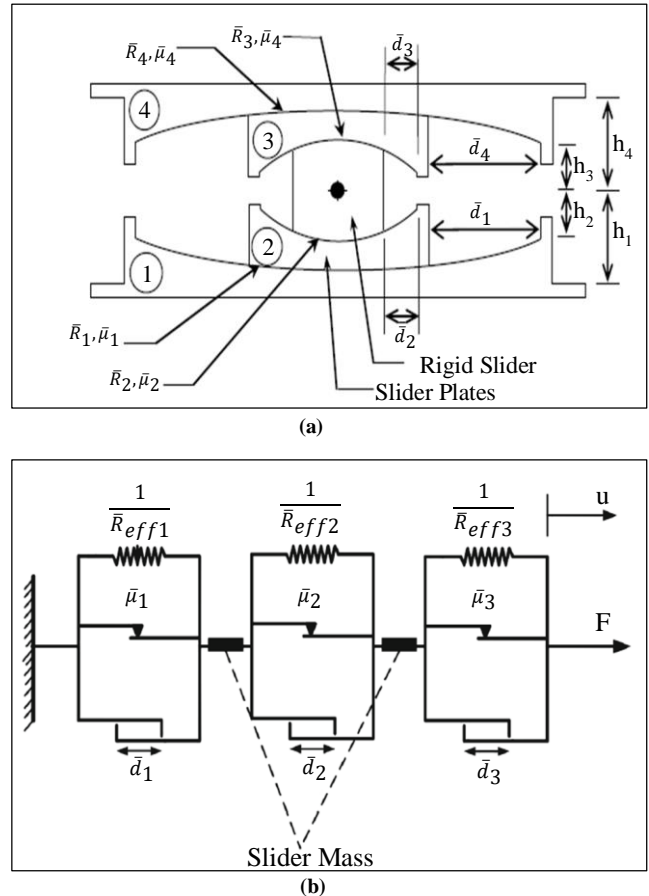


Fig. 1 Triple friction bearing: (a) Schematic diagram (Fenz and Constantine, 2008), and (b) Series model.

**Table 1. The parameters needed to model TFP bearings using the three SFPB elements [5]**

	Effective Radius of Curvature	Coefficient of Friction	Displacement Capacity	Rate Parameter
Element 1	$R_{eff,1} = \bar{R}_{eff,2} + \bar{R}_{eff,3}$	$\mu_1 = \bar{\mu}_2 = \bar{\mu}_3$	$d_1 = \frac{(\bar{d}_1 + \bar{d}_2 + \bar{d}_3 + \bar{d}_4)}{-(d_2 + d_3)}$	$a_1 = \frac{1}{2} \frac{\bar{a}_2 + \bar{a}_3}{2}$
Element 2	$R_{eff,2} = \bar{R}_{eff,1} - \bar{R}_{eff,2}$	$\mu_2 = \bar{\mu}_1$	$d_2 = \frac{\bar{R}_{eff,1} - \bar{R}_{eff,2}}{\bar{R}_{eff,1}} \bar{d}_1$	$a_2 = \frac{\bar{R}_{eff,1}}{\bar{R}_{eff,1} - \bar{R}_{eff,2}} \bar{a}_1$
Element 3	$R_{eff,3} = \bar{R}_{eff,4} - \bar{R}_{eff,3}$	$\mu_3 = \bar{\mu}_4$	$d_3 = \frac{\bar{R}_{eff,4} - \bar{R}_{eff,3}}{\bar{R}_{eff,4}} \bar{d}_4$	$a_3 = \frac{\bar{R}_{eff,4}}{\bar{R}_{eff,4} - \bar{R}_{eff,3}} \bar{a}_4$

The series model is illustrated in Figure 1(b) and comprises three single Friction Pendulum (FP) elements coupled in series. Each FP element, in turn, comprises three distinct elements connected in parallel: Linear spring, frictional element dependent on slider velocity, and gap element to model the displacement capacities.

The stiffness of linear spring is determined by the effective radius of curvature, which is equal to  $\bar{R}_{eff,i} = \bar{R}_i - h_i$ . The other essential parameters for simulating three FP elements ( $R_{eff,i}$ ,  $\mu_i$ ,  $d_i$  and  $a_i$ ) should be chosen following Table 1 to get the adaptive behaviour of TFP bearings [4]. As a result, the force exerted by each isolator element is given by Equation 1,

$$\begin{Bmatrix} F_{xi} \\ F_{yi} \end{Bmatrix} = \begin{bmatrix} \frac{w}{R_{eff,i}} & 0 \\ 0 & \frac{w}{R_{eff,i}} \end{bmatrix} \begin{Bmatrix} u_{xi} \\ u_{yi} \end{Bmatrix} + \begin{bmatrix} \mu_i W_i & 0 \\ 0 & \mu_i W_i \end{bmatrix} \begin{Bmatrix} Z_{xi} \\ Z_{yi} \end{Bmatrix} + \begin{Bmatrix} F_{dxi} \\ F_{dyi} \end{Bmatrix} \quad (1)$$

$W$  is the isolator-supported mass, and the relative displacement of single FP element  $i$  is indicated as  $u_{xi}$  and  $u_{yi}$  in the orthogonal directions. Here,  $\mu_i$  is the  $i^{\text{th}}$  sliding surface's velocity-dependent coefficient of friction, which is given by Equation 2.

$$\mu_i = \mu_{max,i} - (\mu_{max,i} - \mu_{min,i})e^{-a|x_i|} \quad (2)$$

The coefficient of sliding friction at the highest and lowest velocities are  $\mu_{max,i}$  and  $\mu_{min,i}$ .  $a_i$  represent the rate parameter that regulates the variance of the friction coefficient [4].  $Z_{xi}$  and  $Z_{yi}$  are the variables that fluctuate gradually as the isolators slide and quickly when the motion reverses, and are governed by the differential Equation 3,

$$q_i \begin{Bmatrix} \dot{Z}_{xi} \\ \dot{Z}_{yi} \end{Bmatrix} = A \begin{bmatrix} 1 & 0 \\ 0 & 1 \end{bmatrix} \begin{Bmatrix} \dot{u}_{xi} \\ \dot{u}_{yi} \end{Bmatrix} - \begin{bmatrix} |Z_{xi}|^2 [\gamma \text{sign}(\dot{u}_{xi} Z_{xi}) + \beta] & Z_{xi} Z_{yi} [\gamma \text{sign}(\dot{u}_{yi} Z_{yi}) + \beta] \\ Z_{xi} Z_{yi} [\gamma \text{sign}(\dot{u}_{xi} Z_{xi}) + \beta] & |Z_{yi}|^2 [\gamma \text{sign}(\dot{u}_{yi} Z_{yi}) + \beta] \end{bmatrix} \begin{Bmatrix} Z_{xi} \\ Z_{yi} \end{Bmatrix} \quad (3)$$

The dimensionless numbers,  $\beta$ ,  $\gamma$ , and  $A$  regulate the shape of the hysteresis response, and  $q$  is the parameter of yield displacement. The suggested values are  $A = 1$ ,  $\beta = 0.9$ ,  $\gamma = 0.1$ ,  $q = 0.25$  mm [4]. According to the Equation 4,  $F_{dxi}$  and  $F_{dyi}$  are the forces produced in the gap element after it contacts the restrainer.

$$F_{di} = K_G (|u_i| - d_i) \text{sgn}(u_i) H(|u_i| - d_i) \quad (4)$$

Where  $H$  stands for the Heaviside step function, and the stiffness following gap closure is denoted by  $K_G$ , is set to a high value.

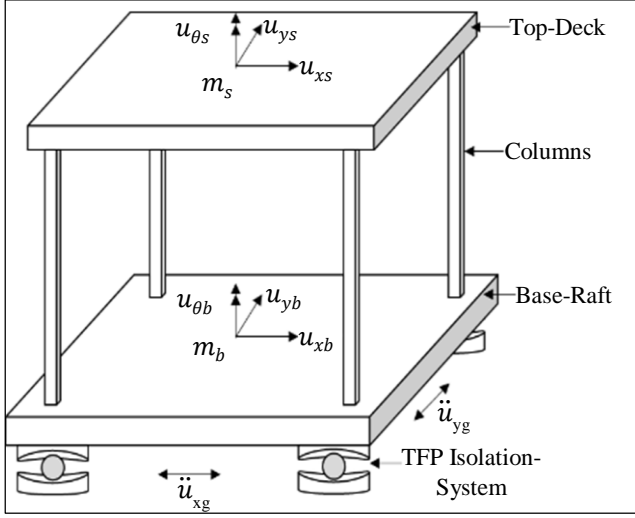
### 3. Structural Modeling and Solution of Equation of Motion

As seen in Figure 2, the TFP base-isolated building is idealized for the current study as a one-story building with concentrated masses at the upper deck and the base raft. Since the isolated structure is anticipated to stay elastic during earthquakes, the structure is modelled as a rigid elastic body. Massless columns are provided at the building's corner; those are attached to a rigid base raft and support the upper deck.

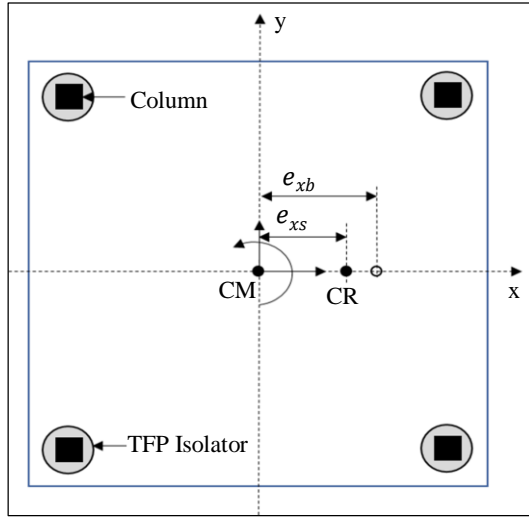
Triple friction pendulum isolators are used to support the base raft. Since the building's mass is thought to be at its geometrical center, eccentricities caused by an uneven distribution of mass are not taken into account.

To study torsional response, the asymmetries in a base-isolated building are taken into consideration at two levels: the isolator level, where they are caused by differences in the stiffness of the isolated systems, and at the superstructure level, where variations in column stiffness cause them. The unidirectional eccentricities are considered at the superstructure and isolator levels to predict how the asymmetric structure would respond.

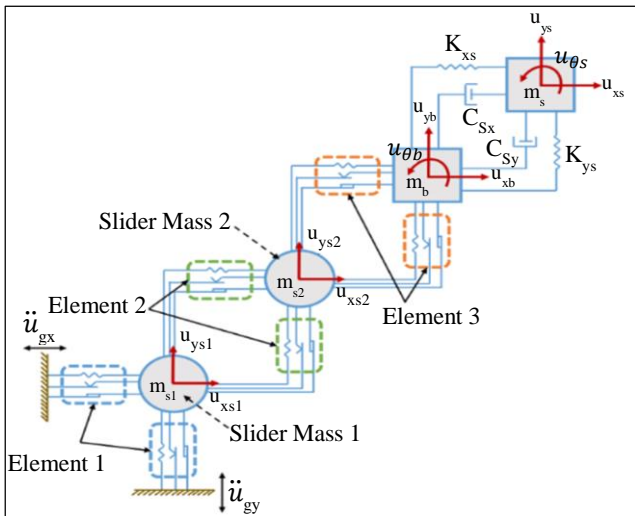
When seismic motions  $\ddot{u}_{xg}$  and  $\ddot{u}_{yg}$  are applied in an orthogonal direction; Equations 5, 6, and 7 represent the equations of motions for the top deck, base raft, and slider isolator level, respectively. The current study has been performed under stochastic ground motion  $\ddot{u}_{xg}$  in x-direction only.



(a)



(b)

**Fig. 2 (a) TFP isolated one-story building, and (b) Eccentricities in the TFP isolated building.**

**Fig. 3 Mathematical model of one-story TFP isolated building**

$$\begin{bmatrix} m_s & 0 & 0 \\ 0 & m_s & 0 \\ 0 & 0 & m_s r_s^2 \end{bmatrix} \begin{Bmatrix} \ddot{u}_{xs} \\ \ddot{u}_{ys} \\ \ddot{u}_{\theta_s} \end{Bmatrix} + [C_s] \begin{Bmatrix} \dot{u}_{xs} \\ \dot{u}_{ys} \\ \dot{u}_{\theta_s} \end{Bmatrix} + \begin{bmatrix} K_{xs} & 0 & -K_{xs} e_{ys} \\ 0 & K_{ys} & K_{ys} e_{xs} \\ -K_{xs} e_{ys} & K_{ys} e_{xs} & K_{\theta_s} \end{bmatrix} \begin{Bmatrix} u_{xs} \\ u_{ys} \\ u_{\theta_s} \end{Bmatrix} = - \begin{bmatrix} m_s & 0 & 0 \\ 0 & m_s & 0 \\ 0 & 0 & m_s r_s^2 \end{bmatrix} \begin{Bmatrix} \ddot{u}_{xb} + \ddot{u}_{xg} \\ \ddot{u}_{yb} + \ddot{u}_{yg} \\ \ddot{u}_{\theta_b} \end{Bmatrix} \quad (5)$$

$$\begin{bmatrix} m_b & 0 & 0 \\ 0 & m_b & 0 \\ 0 & 0 & m_b r_b^2 \end{bmatrix} \begin{Bmatrix} \ddot{u}_{xb} \\ \ddot{u}_{yb} \\ \ddot{u}_{\theta_b} \end{Bmatrix} + \begin{Bmatrix} F_{xb} \\ F_{yb} \\ F_{\theta_b} \end{Bmatrix} - [C_s] \begin{Bmatrix} \dot{u}_{xs} \\ \dot{u}_{ys} \\ \dot{u}_{\theta_s} \end{Bmatrix} - \begin{bmatrix} K_{xs} & 0 & -K_{xs} e_{ys} \\ 0 & K_{ys} & K_{ys} e_{xs} \\ -K_{xs} e_{ys} & K_{ys} e_{xs} & K_{\theta_s} \end{bmatrix} \begin{Bmatrix} u_{xs} \\ u_{ys} \\ u_{\theta_s} \end{Bmatrix} = - \begin{bmatrix} m_b & 0 & 0 \\ 0 & m_b & 0 \\ 0 & 0 & m_b r_b^2 \end{bmatrix} \begin{Bmatrix} \ddot{u}_{xg} \\ \ddot{u}_{yg} \\ 0 \end{Bmatrix} \quad (6)$$

$$\begin{bmatrix} m_{s2} & 0 \\ 0 & m_{s2} \end{bmatrix} \begin{Bmatrix} \ddot{u}_{xs2} \\ \ddot{u}_{ys2} \end{Bmatrix} + \begin{bmatrix} k_{s2} & 0 \\ 0 & k_{s2} \end{bmatrix} \begin{Bmatrix} u_{xs2} \\ u_{ys2} \end{Bmatrix} + \begin{Bmatrix} F_{xs2} \\ F_{ys2} \end{Bmatrix} - \begin{bmatrix} k_{s3} & 0 \\ 0 & k_{s3} \end{bmatrix} \begin{Bmatrix} u_{xs3} \\ u_{ys3} \end{Bmatrix} - \begin{Bmatrix} F_{xs3} \\ F_{ys3} \end{Bmatrix} = - \begin{bmatrix} m_{s2} & 0 \\ 0 & m_{s2} \end{bmatrix} \begin{Bmatrix} \ddot{u}_{xg} \\ \ddot{u}_{yg} \end{Bmatrix} \quad (7)$$

Where  $u_{xb}$  and  $u_{yb}$  are represent the relative base displacements in x and y directions. While relative superstructure displacements are expressed as  $u_{xs}$  and  $u_{ys}$ . The superstructure's torsional displacement is given as  $u_{\theta_s} = r_s \theta_s$ , where  $\theta_s$  denotes rotation.  $[C_s]$  is the superstructure damping matrix [12, 13].

The classical modal superposition approach is unsuitable for solving the equations of motion of the TFP-isolated building due to nonlinear hysteresis behaviour and substantial variation in the superstructure's damping [3]. As a result, the state-space approach is used to solve the equations of motion. The equation of motion (Equation 8 and 9) for the system can be represented by rearranging the equations mentioned above,

$$\{\dot{x}\} = [A]\{x\} + \{B\} \quad (8)$$

Where the vector  $\{x\}$  is,

$$\{x\} = \{u_{s1x} \quad u_{s2x} \quad u_{bx} \quad u_{sx} \quad u_{s1y} \quad u_{s2y} \quad u_{by} \quad u_{sy} \quad \dots \\ u_{b\theta} \quad u_{s\theta} \quad \dot{u}_{s1x} \quad \dot{u}_{s2x} \quad \dot{u}_{bx} \quad \dot{u}_{sx} \quad \dot{u}_{s1y} \quad \dot{u}_{s2y} \quad \dots \\ \dot{u}_{by} \quad \dot{u}_{sy} \quad \dot{u}_{b\theta} \quad \dot{u}_{s\theta} \quad Z_{s1x} \quad Z_{s2x} \quad Z_{s3x} \quad Z_{s1y} \quad \dots \\ Z_{s2y} \quad Z_{s3y} \quad \}^T \quad (9)$$

The above ordinary differential equations are solved simultaneously by using the fourth-order Runge-Kutta method to obtain the response of the TFP-isolated building, and for that, a computer code was created.

#### 4. Stochastic Ground Motion Simulation

Both in the temporal and frequency domains, earthquake motions exhibit nonstationary properties. For the current research, the stochastic model proposed by Rezaeian and Kiureghian [17] addresses the nonstationary nature of earthquake motion is employed. This model accounts for motion's spectral and temporal non-stationarities. These can be incorporated by modifying the intensity and changing filter characteristics over time. The stochastic acceleration's  $[\ddot{x}(t)]$  overall duration is discretized into N steps in this model and then is given by Equation 10,

$$\ddot{x}(t) = q(t) \sum_{i=1}^k a_i(t) w_i, \text{ for } t_k \leq t \leq t_{k+1} \quad (10)$$

Where  $a_i(t)$  are the function that regulates the excitation's frequency content, and the modulation function  $q(t)$  determines the change in excitation amplitude.  $w_i$  are an array of standard normal variables. The four-parameter piecewise modulating function proposed by Dabaghi and Kiureghian [2] is considered and stated in Equation 11,

$$q(t) = \begin{cases} 0 & \text{for } t < t_0 \\ c \left( \frac{t-t_0}{t_{max}-t_0} \right)^\alpha & \text{for } t_0 < t < t_{max} \\ c \exp[-\beta(t-t_{max})] & \text{for } t_{max} < t \end{cases} \quad (11)$$

This modulating function has two phases: sharper build up and decay phases, without a quasi-stationary stage in between. The sharper build-up phase that takes the shape of an order-polynomial from time  $t_0$  to its maximum amplitude  $c$  at  $t_{max}$ , and a decay phase that takes the shape of an exponential function decreasing at a rate of  $\beta$ . The filter function is given by Equation 12,

$$a_i(t) = \frac{h[t-t_i, \omega_f(t_i), \xi_f(t_i)]}{\sqrt{\sum_{j=1}^k h^2[t-t_i, \omega_f(t_i), \xi_f(t_i)]}}, \text{ for } t_k \leq t \leq t_{k+1} \text{ and } 0 < i \leq k \quad (12)$$

The function  $h[t-t_i, \omega_f(t_i), \xi_f(t_i)]$  the response of a single degree of freedom linear oscillator under unit impulse

represents the soil medium through which the earthquake waves transmit. According to Equation 13, this impulse response function is expressed as a function of time  $\tau$ .

$$h[t-t_i, \omega_f(t_i), \xi_f(t_i)] = \begin{cases} \frac{\omega_f(\tau)}{\sqrt{1-\zeta_f^2(\tau)}} e^{-\zeta_f(\tau)\omega_f(\tau)(t-\tau)} \sin \left[ \omega_f(\tau) \sqrt{1-\zeta_f^2(\tau)} (t-\tau) \right]; & \text{for } \tau \leq t \\ 0 & ; \text{for } \tau > t \end{cases} \quad (13)$$

Where  $\omega_f(\tau)$  and  $\zeta_f(\tau)$  are time-varying frequency and damping ratio of the impulse response function. The filter's frequency is thought to degrade linearly as,  $\omega_f(\tau) = \omega_{mid} + \omega'(\tau - t_{mid})$ , with  $\omega'$  indicates the rate of alteration of the filter frequency over time and  $\omega_{mid}$  representing the filter frequency at  $t_{mid}$ .

Therefore, the process that represents the broadband ground acceleration is thus entirely defined by the eight significant parameters ( $\alpha, \beta, c, t_{max}, t_0, \omega_{mid}, \omega', \zeta_f$ ). Out of this, five parameters ( $\alpha, \beta, c, t_{max}, t_0$ ) form the time modulation function and are coupled to three physically-based parameters ( $I_a, D_{5-95}, t_{mid}$ ). These eight parameters can be discovered by comparing the characteristics of the observed ground motion with the relevant statistical measurements of the stochastic ground motion model.

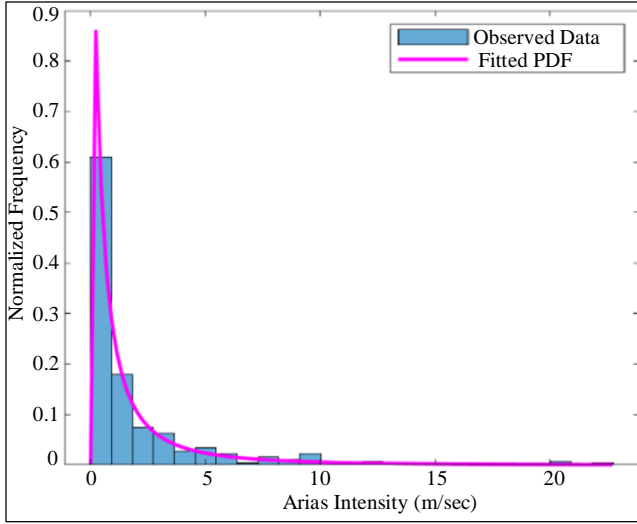
A thorough methodology for determining the stochastic parameters and producing stochastic ground motions was described by Rezaeian and Kiureghian [17] and Dabaghi and Kiureghian [2]. A total of 280 ground motions are considered to identify modal parameters. After determining the model parameters by matching them to each recorded motion in the database, a probability distribution is allocated to the sample of values of each parameter.

The resulting histograms for the determined parameters and the Fitted Probability Distribution (PDF) are displayed in Figure 4. By means of Monte Carlo (MC) simulation, a pool of synthetic stochastic ground motion is produced based on the allocated PDF of the input parameters. The characteristics of the 1000 earthquake motions that were generated are summarized in Table 2.

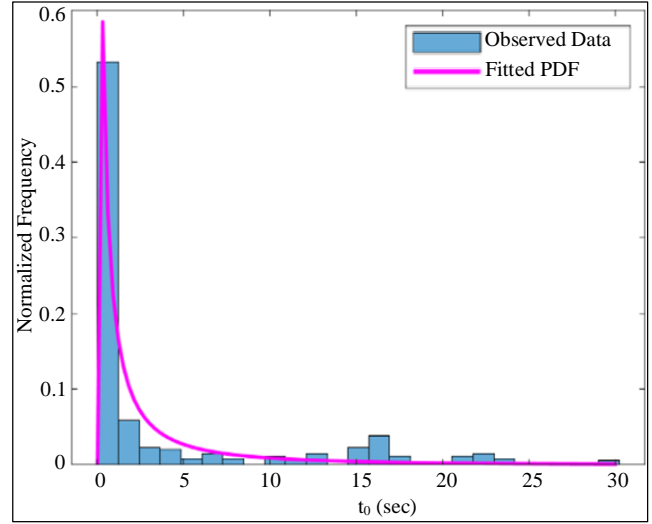
Table 2. Characteristics of generated stochastic ground motions

Earthquake Characteristics	Minimum	Maximum	Mean	Standard Deviation
Peak Ground Acceleration (g)	0.0717	1.5965	0.3344	0.221
Frequency <sup>a</sup> (Hz)	0.03	106.78	30.29	18.52
Duration (sec)	2.50	115.28	30.477	17.169

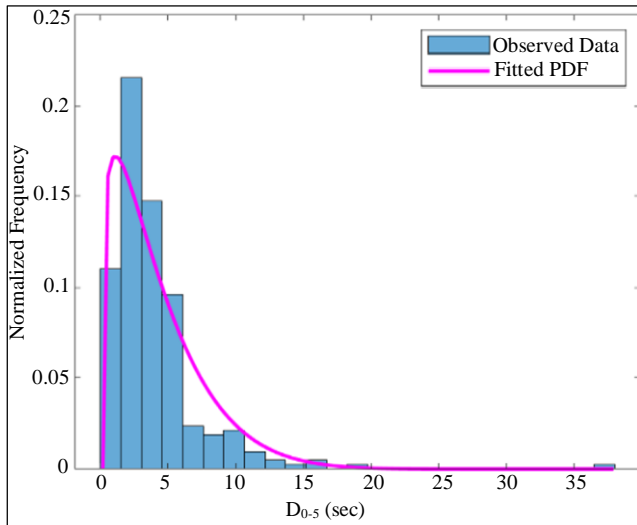
<sup>a</sup> - related to the maximum FFT amplitude of generated motion



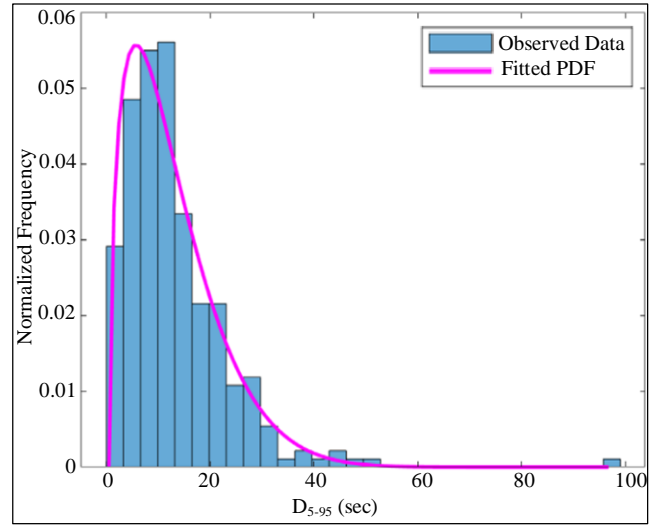
(a) Lognormal distribution of arias intensity



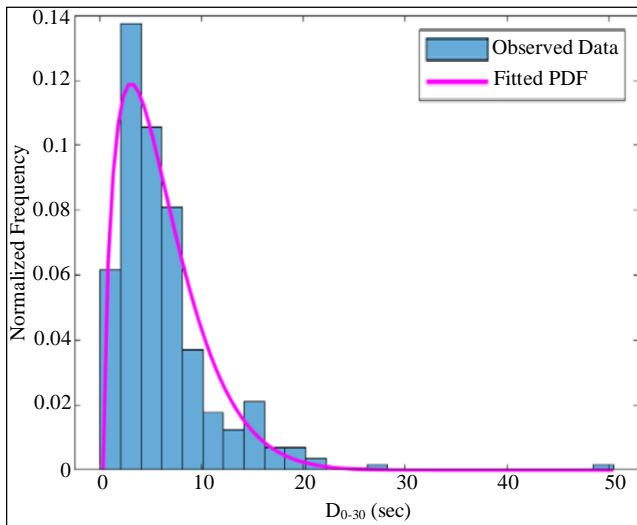
(b) Lognormal distribution for  $t_0$



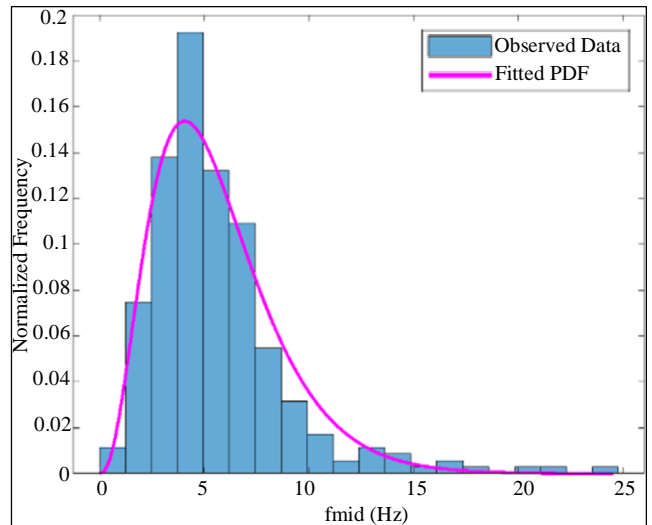
(c) Beta distribution for  $D_{0.5}$



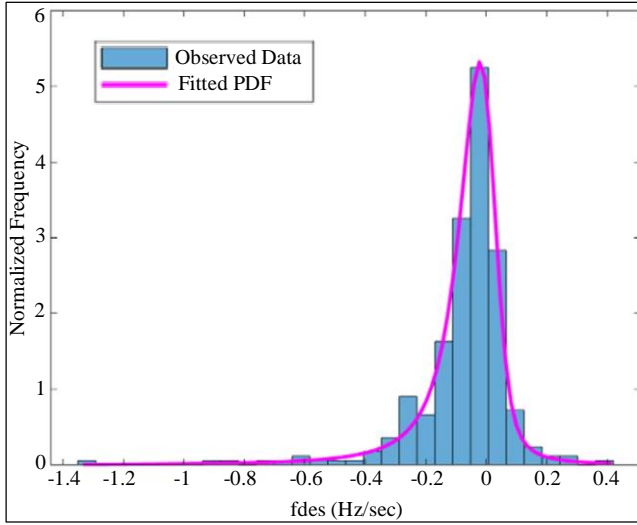
(d) Beta distribution for  $D_{5.95}$



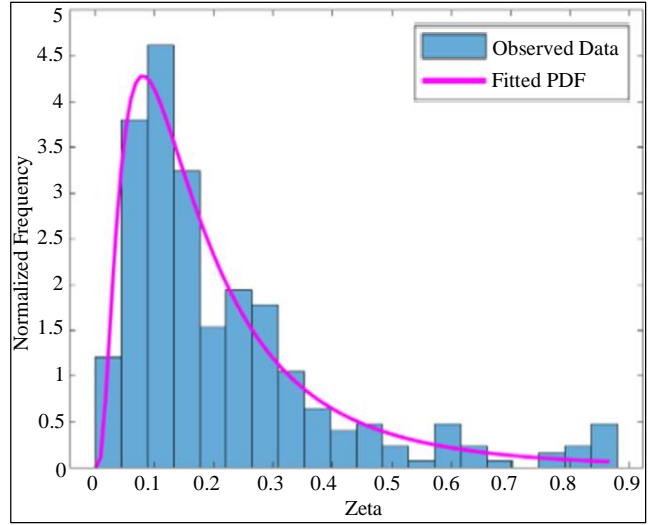
(e) Beta distribution for  $D_{0.30}$



(f) Gamma distribution for  $\omega_{mid}$



(g) Stable distribution for  $\omega'$

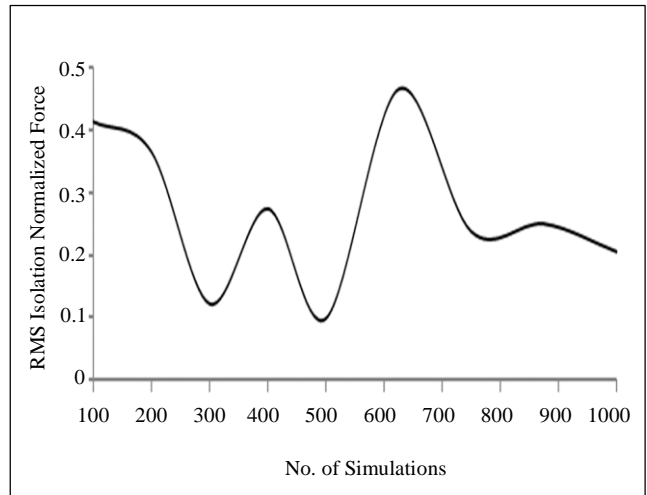
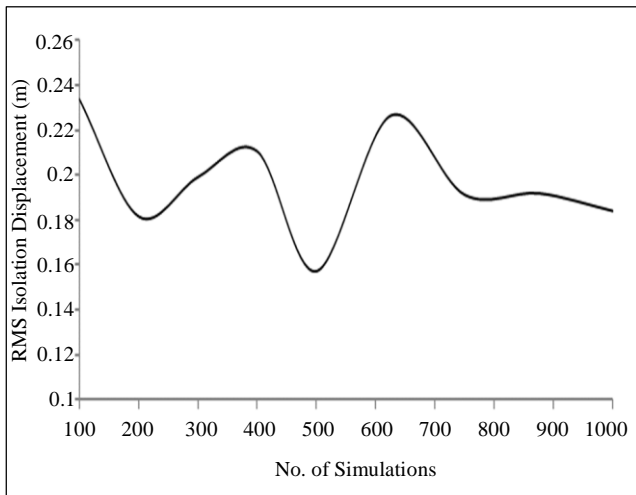
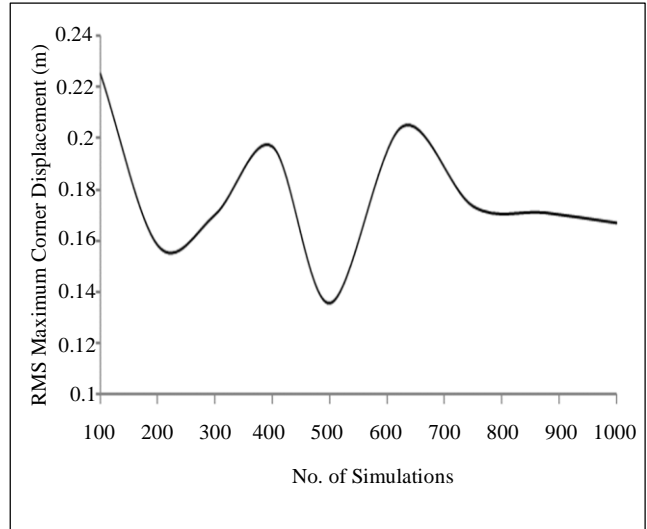


(h) Lognormal distribution for  $\zeta_f$

Fig. 4 Histograms for the model parameters and fitted PDFs

### 5. Convergence under Stochastic Ground Motion

The number of simulations is crucial when utilizing the MC simulation to identify the response. A significant number of simulations increases computation time, and a limited number of simulations can affect accuracy. Therefore, a convergence study determines the number of stochastic ground motions essential to estimate the isolated building response with reasonable accuracy and time [19]. A series of probabilistic ground motions are simulated to conduct a convergence study, and then a deterministic analysis is performed for each simulation. Figure 5 depicts the response versus the number of simulations for the torsionally coupled isolated building. It has been found that 1000 simulations are enough to reasonably predict the torsional behavior of a remote building. Hence, based on this study, 1000 stochastic ground motions are selected for all analyses now presented.



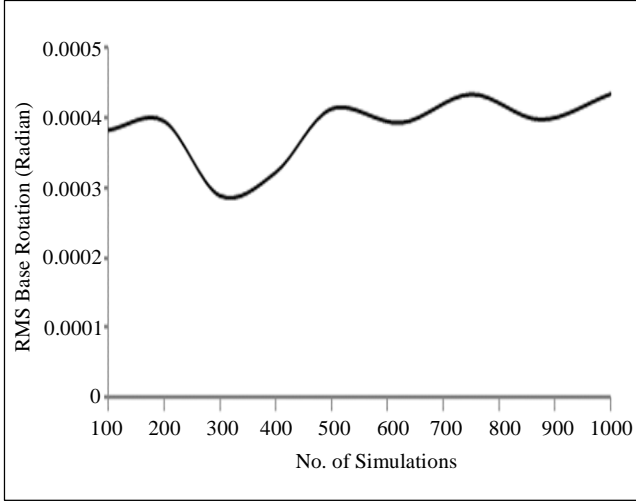
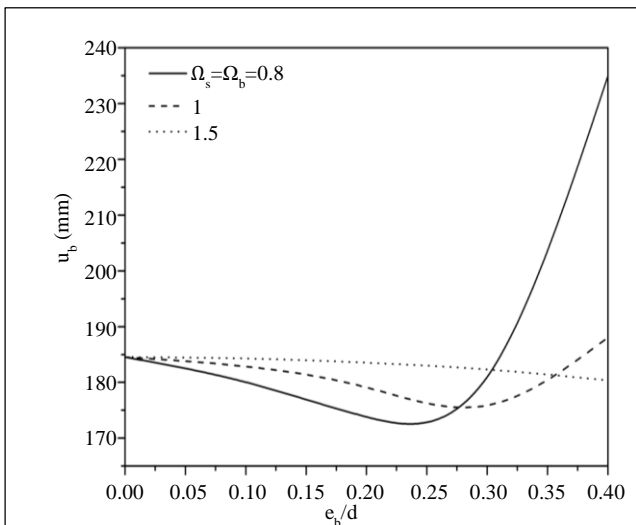


Fig. 5 Convergence of response (RMS) quantity with the number of simulations for torsional response

### 6. Torsional Response of a TFP Isolated Building under Stochastic Ground Motion

Under stochastic ground motions, the seismic response of an asymmetric building resting on a triple friction isolation bearing is studied. For the investigation, asymmetry is only considered in the x-direction. The uncoupled torsional to lateral frequency ratio of the superstructure ( $\Omega_s$ ), uncoupled torsional to lateral frequency ratio of isolator ( $\Omega_b$ ), ratio of superstructure eccentricity ( $\frac{e_s}{d}$ ), the ratio of base eccentricity ( $\frac{e_b}{d}$ ), are the torsional parameters that mainly influence the torsional response of the TFP-isolated structures. Therefore, a parametric variation of these parameters is considered to examine the influence of these parameters on torsional response. The frequency ratio is the most crucial factor affecting the structure’s torsional behaviour, which is considered as  $\Omega_s = \Omega_b = 0.8, 1, \text{ and } 1.5$ . A higher frequency ratio signifies a torsionally rigid structure.

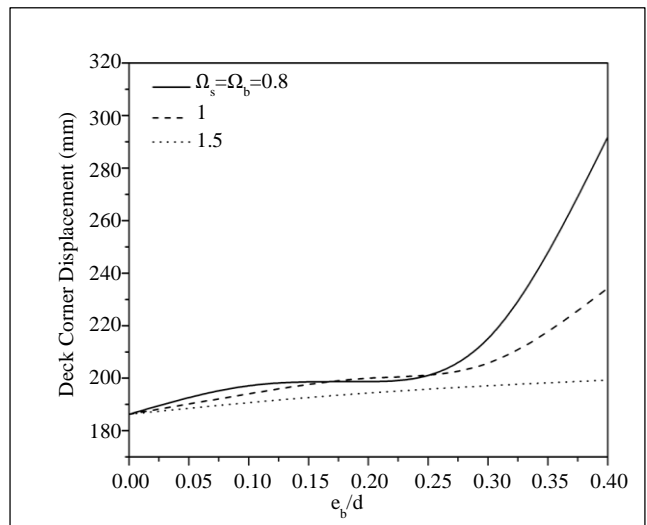


This torsional response study is performed on a building with a plan dimension ratio ( $b/d$ ) as 1 representing square configuration. The lateral plan dimensions  $b=d=10\text{m}$  are considered to avoid chances of uplift. The numerical value for other constant parameters of the isolator and structure are considered as; base mass to floor mass ( $m_b/m_s$ ) =1, isolator slider mass to floor mass =0.001, Time period of the superstructure ( $T_s$ ) = 0.2 sec and Damping factor = 0.02.

To understand the torsional response of a base-isolated system, response parameters considered are lateral displacement at the base level, deck corner displacement, base rotation, normalized base torsion, normalized base shear, and deck corner displacement magnification. Deck corner displacement magnification is computed by comparing maximum deck corner displacement to maximum deck lateral displacement. The deck corner magnification factor is used to subjectively assess the impact of torsional coupling since it reflects the extent of deformation induced by the collective influence of torsion and translation.

#### 6.1. Influence of Base Eccentricity

Under stochastic ground motions, Figure 6 shows the response of a triple friction isolated structure to the isolation eccentricity ratio, ( $\frac{e_b}{d}$ ). The superstructure unidirectional eccentricity ratio is held constant at zero. ( $\frac{e_s}{d} = 0$ ). It has been found that when isolator eccentricity increases, the lateral displacement marginally decreases. Compared to the uncoupled scenario, the torsional and corner displacements rise with increased isolator eccentricity. The torsional response is amplified when a system is torsionally flexible instead of rigid. However, the frequency ratio does not significantly impact base shear and bearing displacement. It is essential to notice that the resonance condition might substantially increase the displacement response for isolation eccentricity ratios. ( $\frac{e_b}{d}$ )=0.4 and frequency ratio = 0.8.



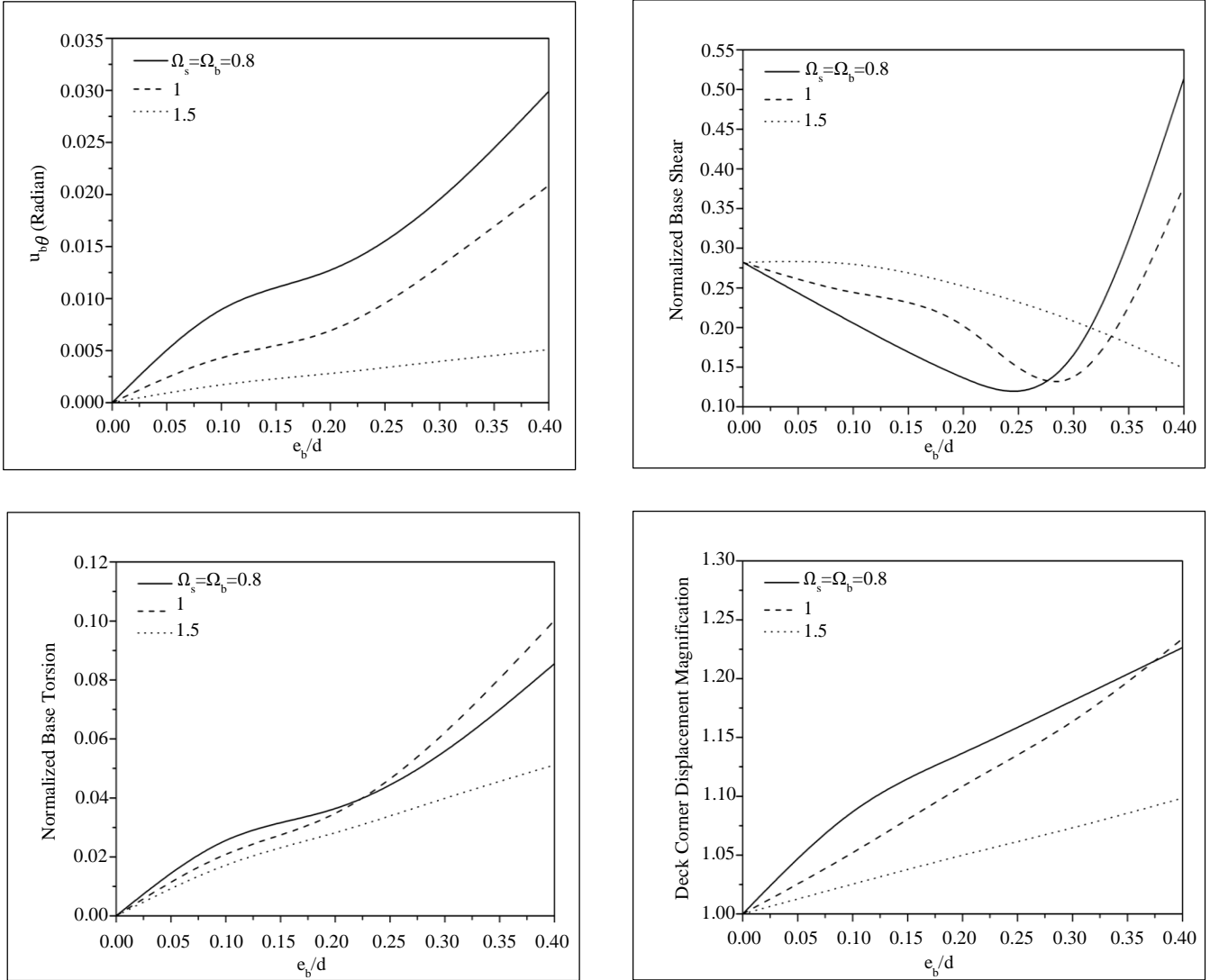
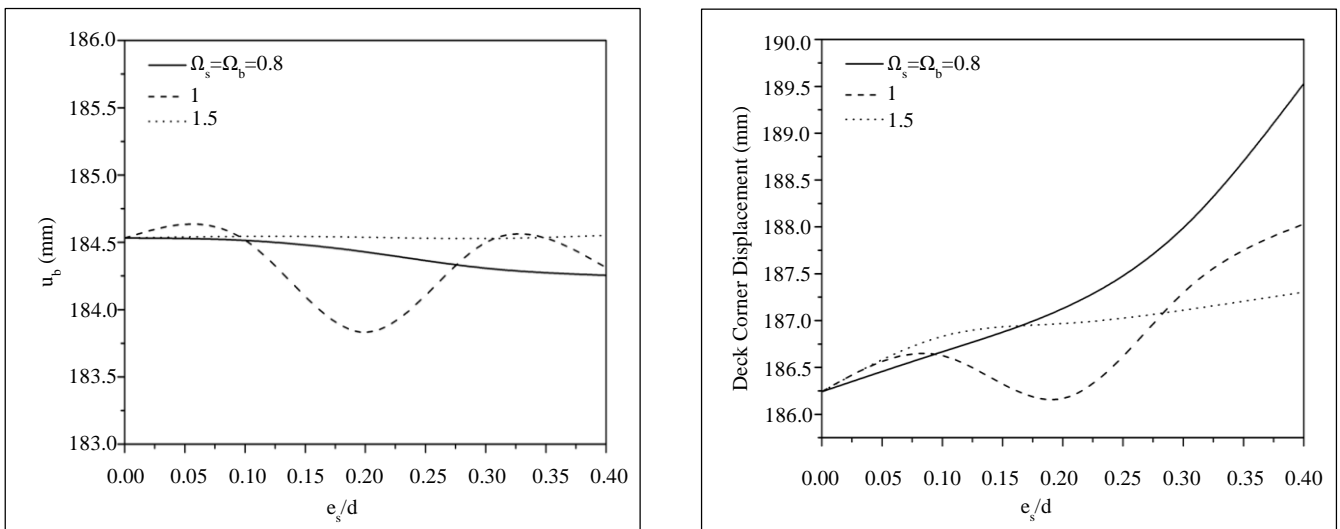


Fig. 6 Influence of base eccentricity ( $\frac{e_b}{d}$ ) on the behaviour of TFP isolated structure



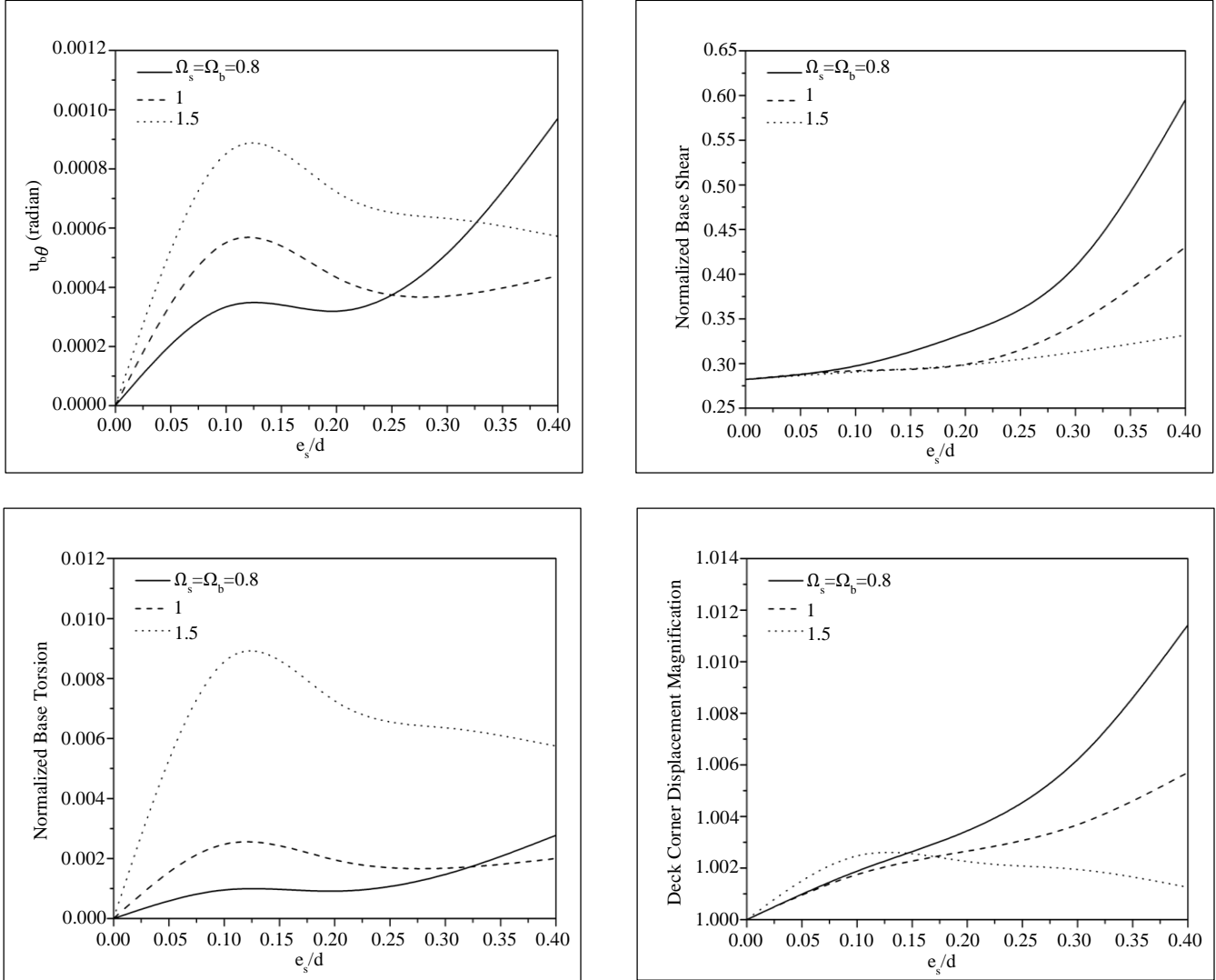


Fig. 7 Influence of superstructure eccentricity ( $\frac{e_s}{d}$ ) on the behaviour of TFP isolated structure

### 6.2. Influence of Superstructure Eccentricity

Superstructure eccentricity is the primary factor driving a structure’s torsional coupling and torsional motion. Keeping the base eccentricity ratio at zero ( $\frac{e_b}{a} = 0$ ), the fluctuation of RMS values of response quantities is displayed against the superstructure eccentricity ratio ( $\frac{e_s}{d}$ ) in Figure 7. It has been found that the displacement response is nearly consistent for all superstructure eccentricity ratios.

Additionally, it has been noted that the eccentricity of the superstructure has very little impact on the base shear normalized by structural weight. That indicates that the torsional behaviour of the TFP-isolated building is less influenced by superstructure eccentricity when the superstructure is rigid. Therefore, examining how eccentric superstructures impact structural behaviour in the presence of

isolated eccentricities is crucial. Figure 8 shows the behaviour of a torsionally coupled TFP isolated structure. The superstructure eccentricity varies from a symmetric case ( $\frac{e_s}{d} = 0$ ), to asymmetric case ( $\frac{e_s}{d} = 0.4$ ), keeping the base eccentricity ratio constant as, ( $\frac{e_b}{a} = -0.3$ ). The base eccentricity ratio with a negative sign indicates the base eccentricity applied in the opposite direction to the superstructure eccentricities.

The displacement response is not considerably altered by the extreme mix of the top deck and base raft eccentricities that were chosen. Additionally, for all eccentricity, the deck corner displacement magnification is constant. This demonstrates that eccentric superstructures have less impact on torsional response.

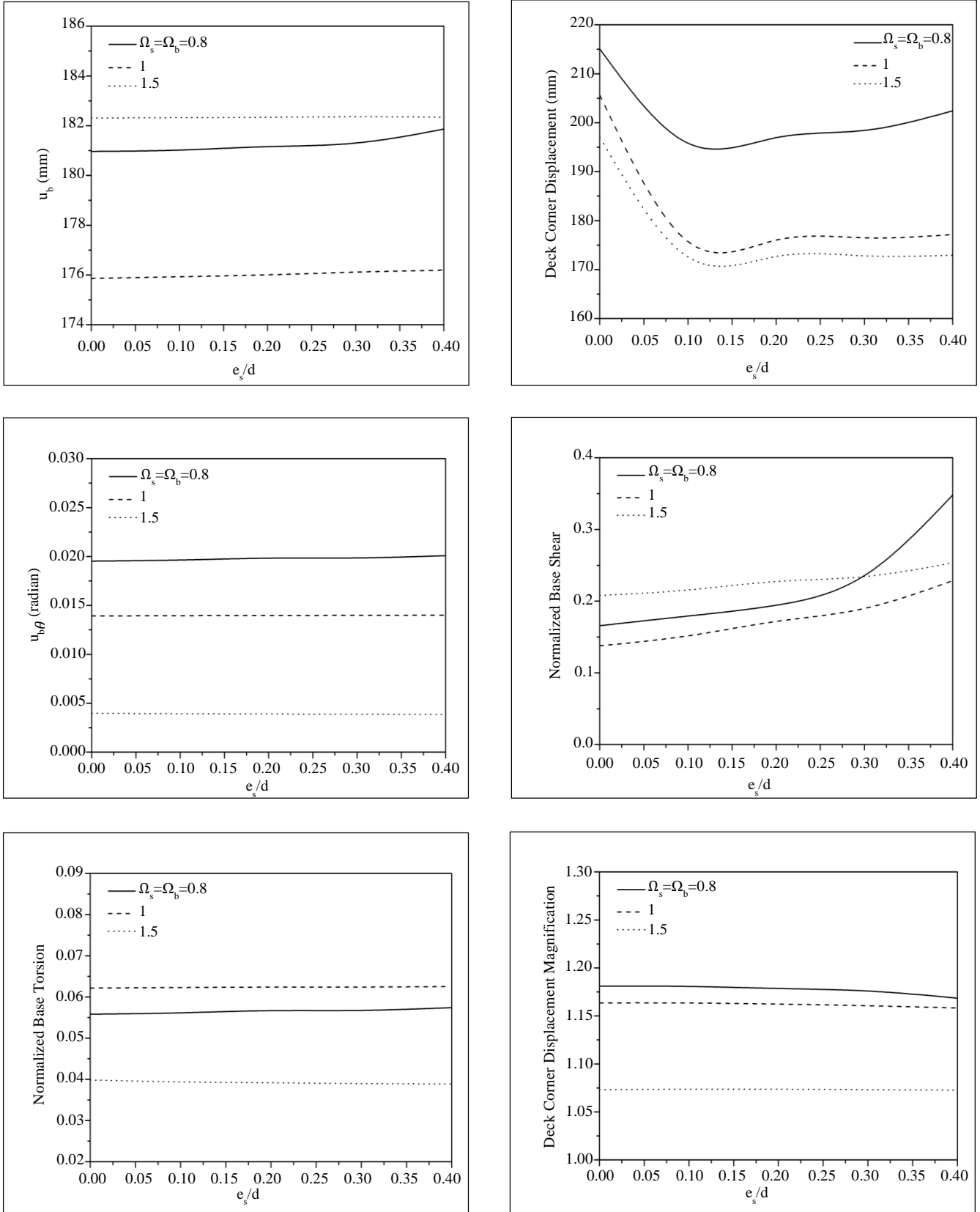


Fig. 8 Influence of superstructure eccentricity ( $\frac{e_s}{d}$ ) along with opposite constant base eccentricity ( $\frac{e_b}{d} = -0.3$ )

**6.3. Influence of Superstructure Flexibility**

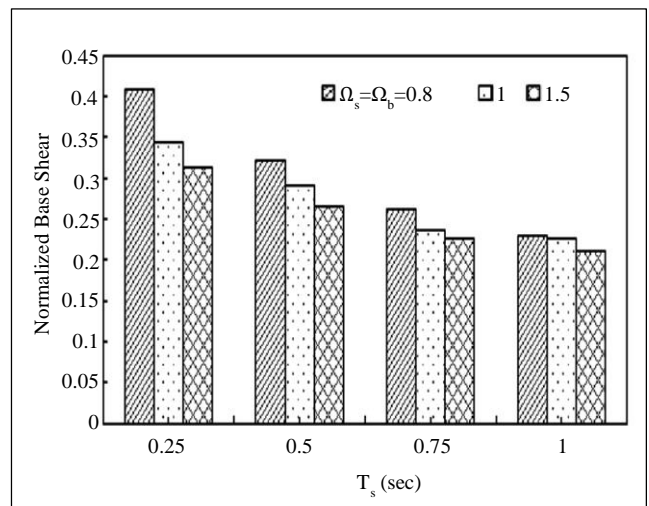
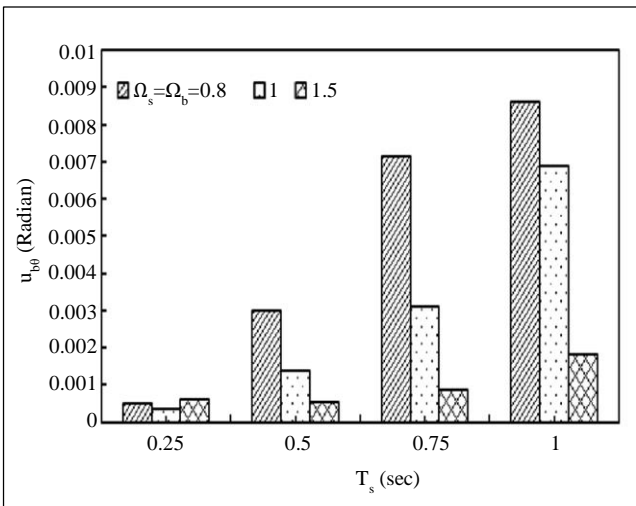
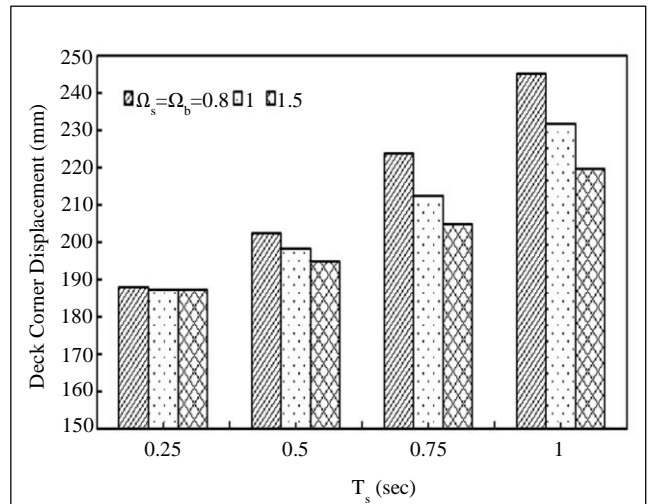
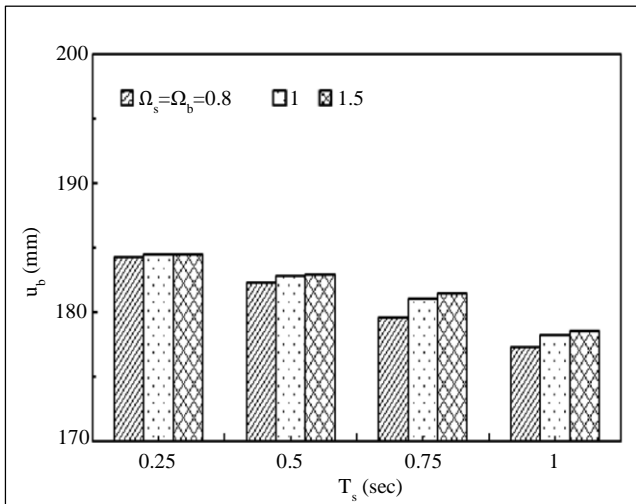
In Figure 9, the behaviour of the TFP Isolated building is plotted for different values of a superstructure time period. This parametric analysis is carried out to determine how the flexibility of the superstructure affects the response of torsionally coupled TFP isolated structures under stochastic ground motion. It has been found that the base-isolated structure’s torsional response is increased with a rise in superstructure flexibility. However, the lateral response is decreased with increased superstructure flexibility, which increases superstructure corner displacement magnification. Therefore, the rise in torsional response is very significant for torsionally flexible structures.

**6.4. Influence of Torsional to Lateral Flexibility Ratio**

Studying the impact of the torsional to lateral frequency ratio on the response of TFP isolated asymmetric systems is more crucial since the response of a torsionally coupled system is strongly influenced by this ratio.

Based on the previous findings, base eccentricity is considered when examining the impact of the torsional to lateral frequency ratio because it has been found to impact the torsional response of TFP isolated structures substantially. Examining the torsional-to-lateral frequency ratio’s combined impact and isolator eccentricity is fascinating and crucial.

Base rotation and normalized base torsion decrease with increasing frequency ratio, as seen in Figure 10, while the lateral response is still unresponsive to changes in frequency ratio. It is evident from Figure 10 that the  $(\frac{e_b}{d})$  and frequency ratio ( $\Omega_b = \Omega_s$ ) have conflicting impacts on the coupled lateral-torsional response of the TFP isolated system. With a rise in base eccentricity, the system’s torsional response increases quickly; the frequency ratio suppresses this response. Therefore, controlling eccentricity is always preferable for controlling the torsion response rather than increasing torsional stiffness.



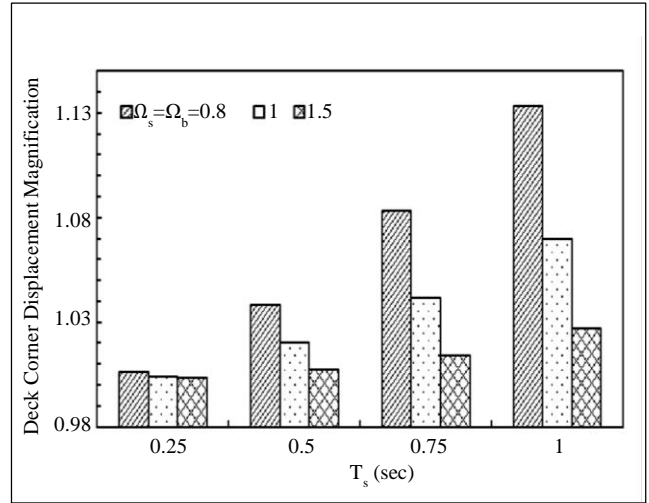
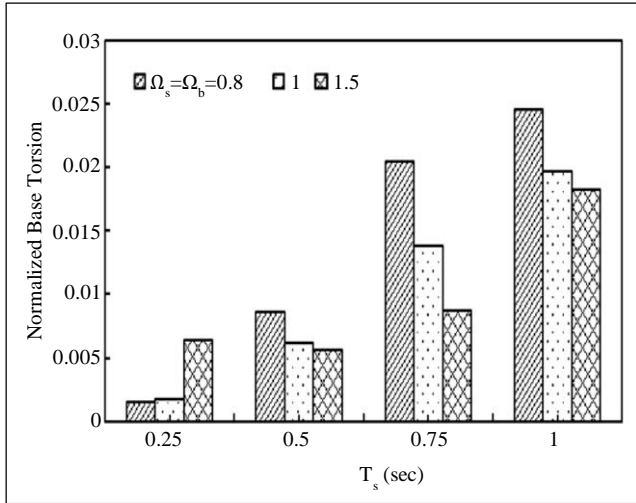
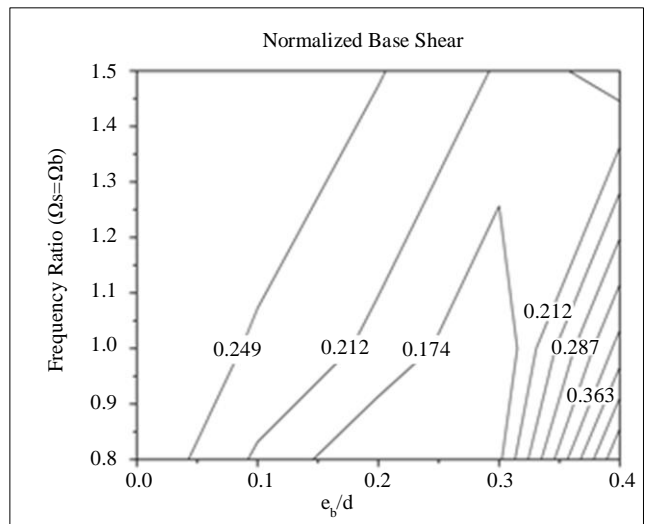
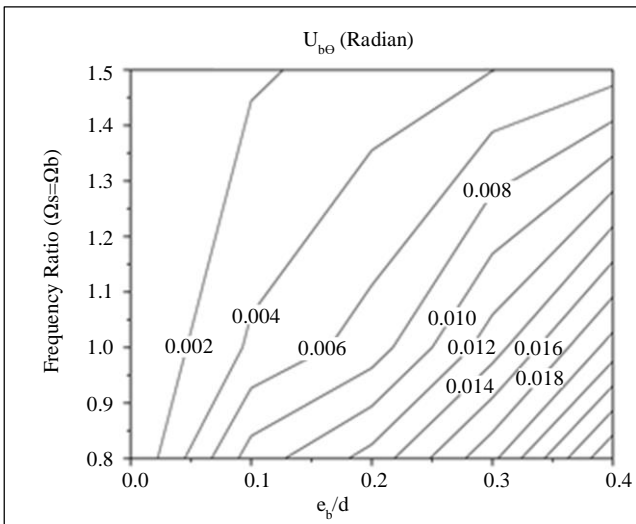
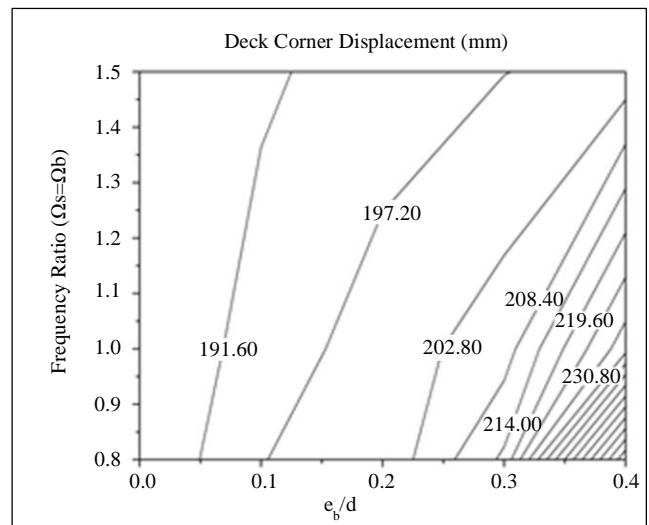
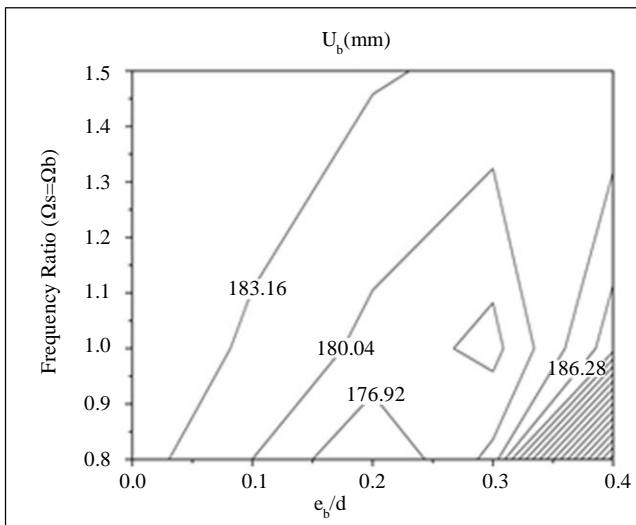


Fig. 9 Influence of superstructure flexibility on the behaviour of TFP isolated structure



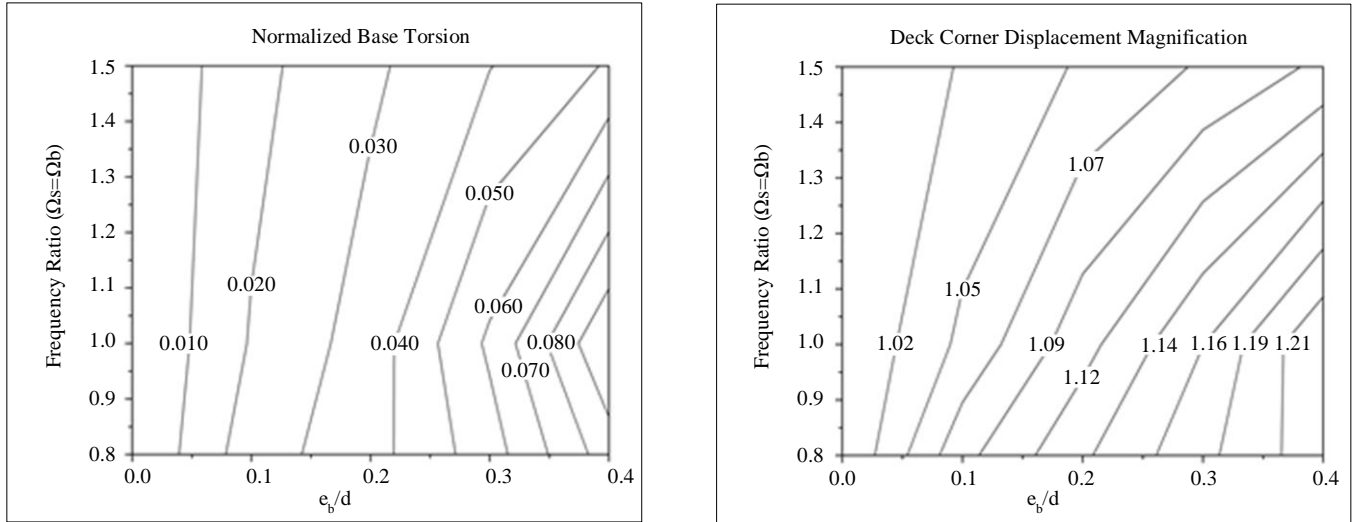


Fig. 10 Combined influence of isolator eccentricity ( $\frac{e_b}{d}$ ) and frequency ratio ( $\Omega_b = \Omega_s$ )

### 6.5. Comparison with Code Recommendation

The expression mentioned in Equation 14 is suggested by the UBC (1997) standard for calculating an additional displacement of the isolator caused by torsion [20]:

$$D_{TM} = D_M \left( 1 + Y \frac{12e}{B^2 + D^2} \right) \quad (14)$$

Where  $D_{TM}$  is the total maximum displacement of the bearing;  $D_M$  is the maximum displacement at the CR of the isolator;  $Y$  represents the corner isolator's distance from the center of rigidity, and  $e$  represents the system's eccentricity, including accidental eccentricity.

Table 3 compares corner bearing displacement obtained under stochastic ground motions to the appropriate UBC (1997) formula for accidental torsion. The corner isolator displacement of the torsionally uncoupled structure is normalized with the lateral displacement for comparative study. Regarding normalized corner bearing displacements, it is observed from the comparison that the torsional response of an isolated TFP building is overestimated by the UBC (1997).

## 7. Conclusion

Under stochastic ground motions, the nonlinear behaviour of a torsionally coupled structure mounted on a TFP isolator is examined. Here, research is conducted on the impact of several significant parameters on the response of a torsionally coupled system. The following findings are the numerical trends of the response of the torsionally coupled TFP isolated building.

1. The isolator eccentricity cannot be disregarded because it substantially impacts the torsional behavior of TFP Isolated structures and worsens with increasing

eccentricity. An increase in response ranging from 10% to 25 % has been observed for the eccentricity ratio.  $\left(\frac{e_b}{d}\right) = 0.4$ .

2. For TFP-isolated systems, lateral displacement and torsional response are less affected by superstructure eccentricity. Even in the torsionally tuned structures, the torsional response is not much impacted. And is ranging from 0.5% to 1.2%.
3. The torsional response of TFP Isolated building is amplified with Superstructure flexibility, whilst the lateral base response and base shear are decreased. Hence, the influence of flexibility of the superstructure is more on the torsional response of TFP Isolated building.
4. In stiff eccentric systems, the base shear remains constant for low eccentricity degrees. Meanwhile, for larger eccentricity values, the base shear escalates from 45% to 67% with an increase in superstructure eccentricity.
5. The rigid superstructure assumption overestimated the superstructure acceleration (Normalised base shear) of the TFP Isolated structure, and this overestimation is observed up to 75% for superstructures having a time period of 1 sec.
6. The torsional response should be effectively controlled by controlling the eccentricity rather than increasing torsional stiffness; as the system's torsional response increases quickly with a rise in base eccentricity, the frequency ratio suppresses them.
7. UBC overestimates the design displacement caused by isolator eccentricities in TFP base-isolated structures proposed by accidental torsion expressions. This overestimation ranges from 36% to 89% for the eccentricity ratio.  $\left(\frac{e_b}{d}\right) = 0.1$  to 0.4.

## References

- [1] Ian G. Buckle et al., "Seismic Isolation: History, Application and Performance-A World Overview," *Earthquake Spectra*, vol. 46, no. 2, pp. 161-201, 1990. [[Google Scholar](#)] [[Publisher Link](#)]
- [2] Mayssa Dabaghi, and Armen Der Kiureghian, "Stochastic Model for Simulation of Near-Fault Ground Motions," *Earthquake Engineering & Structural Dynamics*, vol. 46, no. 6, 2017. [[CrossRef](#)] [[Google Scholar](#)] [[Publisher Link](#)]
- [3] Mazhar A. Dhankot, and Devesh P. Soni, "Seismic Response of Triple Friction Pendulum Bearing under Multi Hazard Level Excitations," *International Journal of Structural Engineering*, vol. 7, no. 4, pp. 412-431, 2016. [[CrossRef](#)] [[Google Scholar](#)] [[Publisher Link](#)]
- [4] Daniel M. Fenz, and Michael C. Constantinou, "Modeling Triple Friction Pendulum Bearings for Response-History Analysis," *Earthquake Spectra*, vol. 24, no. 4, pp. 1011-1028, 2008. [[Google Scholar](#)] [[Publisher Link](#)]
- [5] Daniel M. Fenz, and Michael C. Constantinou, "Spherical Sliding Isolation Bearings with Adaptive Behavior: Theory," *Earthquake Engineering & Structural Dynamics*, vol. 37, no. 2, pp. 163-183, 2008. [[CrossRef](#)] [[Google Scholar](#)] [[Publisher Link](#)]
- [6] R.S. Jangid, "Seismic Response of an Asymmetric Base-Isolated Structure," *Computers and Structures*, vol. 60, no. 2, pp. 261-267, 1996. [[CrossRef](#)] [[Google Scholar](#)] [[Publisher Link](#)]
- [7] R.S. Jangid, and T.K. Datta, "Non-Linear Response of Torsionally Coupled Base-Isolated Structure," *Journal of Structural Engineering*, vol. 120, no. 1, pp. 1-22, 1994. [[CrossRef](#)] [[Google Scholar](#)] [[Publisher Link](#)]
- [8] R.S. Jangid, and T.K. Datta, "Seismic Response of Torsionally Coupled Structure with Elasto-Plastic Base Isolation," *Engineering Structures*, vol. 16, no. 4, pp. 256-262, 1994. [[CrossRef](#)] [[Google Scholar](#)] [[Publisher Link](#)]
- [9] R.S. Jangid, and T.K. Datta, "Seismic Behaviour of Base Isolated Buildings: A State-of-the-Art Review," *Structures and Buildings*, vol. 110, no. 2, pp. 186-203, 1995. [[CrossRef](#)] [[Google Scholar](#)] [[Publisher Link](#)]
- [10] R.S. Jangid, and T.K. Datta, "Performance of Base Isolation Systems for Asymmetric Building Subject to Random Excitation," *Engineering Structures*, vol. 17, no. 6, pp. 443-454, 1995. [[CrossRef](#)] [[Google Scholar](#)] [[Publisher Link](#)]
- [11] R.S. Jangid, and T.K. Datta, "The Stochastic Response of Asymmetric Base-Isolated Buildings," *Journal of Sound and Vibration*, vol. 179, no. 3, pp. 463-473, 1995. [[CrossRef](#)] [[Google Scholar](#)] [[Publisher Link](#)]
- [12] Vasant A. Matsagar, and R.S. Jangid, "Base-Isolated Building with Asymmetries Due to the Isolator Parameters," *Advances in Structural Engineering*, vol. 8, no. 6, pp. 603-621, 2005. [[CrossRef](#)] [[Google Scholar](#)] [[Publisher Link](#)]
- [13] V.A. Matsagar, and R.S. Jangid, "Impact Response of Torsionally Coupled Base Isolated Structure," *Journal of Vibration and Control*, vol. 16, no. 11, pp. 1623-1649, 2010. [[CrossRef](#)] [[Google Scholar](#)] [[Publisher Link](#)]
- [14] Farzad Naeim, and James M. Kelly, *Design of Seismic Isolated Structures: From Theory to Practice*, John Wiley & Sons, Inc, New York, 1999. [[CrossRef](#)] [[Google Scholar](#)] [[Publisher Link](#)]
- [15] Satish Nagarajaiah, and Xiaohong Sun, "Base-Isolated FCC Building: Impact Response in Northridge Earthquake," *Journal of Structural Engineering*, vol. 127, no. 9, pp. 1063-1075, 2001. [[CrossRef](#)] [[Google Scholar](#)] [[Publisher Link](#)]
- [16] Sanaz Rezaeian, and Armen Der Kiureghian, "Simulation of Synthetic Ground Motions for Specified Earthquake and Site Characteristics," *Earthquake Engineering & Structural Dynamics*, vol. 39, no. 10, pp. 1155-1180, 2010. [[CrossRef](#)] [[Google Scholar](#)] [[Publisher Link](#)]
- [17] Sanaz Rezaeian, and Armen Der Kiureghian, "Stochastic Ground Motion Model with Separable Temporal and Spectral Nonstationarities," *Earthquake Engineering & Structural Dynamics*, vol. 37, no. 13, pp. 1565-1584, 2008. [[CrossRef](#)] [[Google Scholar](#)] [[Publisher Link](#)]
- [18] D.P. Soni, B.B. Mistry, and V.R. Panchal, "Behaviour of Asymmetric Building with Double Variable Frequency Pendulum Isolator," *Structural Engineering and Mechanics*, vol. 34, no. 1, pp. 61-84, 2010. [[CrossRef](#)] [[Google Scholar](#)] [[Publisher Link](#)]
- [19] Sandip Kumar Saha, Vasant A. Matsagar, and Arvind K. Jain, "Seismic Fragility of Base-Isolated Water Storage Tanks under Non-Stationary Earthquakes," *Bulletin of Earthquake Engineering*, vol. 14, no. 4, pp. 1153-1175, 2016. [[CrossRef](#)] [[Google Scholar](#)] [[Publisher Link](#)]
- [20] ICBO -1997, Uniform Building Code, International Conference of Building Officials, Whittier, California, 1997. [Online]. Available: [https://webstore.ansi.org/preview-pages/ICBO/preview\\_ICBO+USC-1997.pdf](https://webstore.ansi.org/preview-pages/ICBO/preview_ICBO+USC-1997.pdf)